JCI The Journal of Clinical Investigation

Differential subunit composition of the G protein–activated inward-rectifier potassium channel during cardiac development

Bernd K. Fleischmann, … , Juergen Hescheler, Bernd Fakler

J Clin Invest. 2004;114(7):994-1001. https://doi.org/10.1172/JCI15925.

Article **Development**

Parasympathetic slowing of the heart rate is predominantly mediated by acetylcholine-dependent activation of the G protein–gated potassium (K^+) channel ($I_{K,ACh}$). This channel is composed of 2 inward-rectifier K^+ (Kir) channel subunits, Kir3.1 and Kir3.4, that display distinct functional properties. Here we show that subunit composition of $I_{K,ACh}$ changes during embryonic development. At early stages, $I_{K,ACh}$ is primarily formed by Kir3.1, while in late embryonic and adult cells, Kir3.4 is the predominant subunit. This change in subunit composition results in reduced rectification of $I_{K,ACh}$, allowing for marked K^+ currents over the whole physiological voltage range. As a consequence, $I_{K,ACh}$ is able to generate the membrane hyperpolarization that underlies the strong negative chronotropy occurring in late- but not early-stage atrial cardiomyocytes upon application of muscarinic agonists. Both strong negative chronotropy and membrane hyperpolarization can be induced in early-stage cardiomyocytes by viral overexpression of the mildly rectifying Kir3.4 subunit. Thus, a switch in subunit composition is used to adopt $I_{K,ACh}$ to its functional role in adult cardiomyocytes.

Differential subunit composition of the G protein–activated inward-rectifier potassium channel during cardiac development

Bernd K. Fleischmann,[1] Yaqi Duan,[2] Yun Fan,[3] Torsten Schoneberg,[4] Andreas Ehlich,[5] Nibedita Lenka,[2] Serge Viatchenko-Karpinski,[2] Lutz Pott,[6] Juergen Hescheler,[2] and Bernd Fakler[7]

[1]Institute of Physiology I, University of Bonn, Bonn, Germany. [2]Institute of Neurophysiology, University of Cologne, Cologne, Germany. [3]Department of Biomedical Engineering, Fourth Military Medical University, Xian, China. [4]Department of Molecular Biochemistry, University of Leipzig, Leipzig, Germany. [5]Axiogenesis AG, Cologne, Germany. [6]Institute of Physiology, Ruhr-University Bochum, Bochum, Germany. [7]Institute of Physiology II, University of Freiburg, Freiburg, Germany.

Parasympathetic slowing of the heart rate is predominantly mediated by acetylcholine-dependent activation of the G protein–gated potassium (K^+) channel ($I_{K,ACh}$). This channel is composed of 2 inward-rectifier K^+ (Kir) channel subunits, Kir3.1 and Kir3.4, that display distinct functional properties. Here we show that subunit composition of $I_{K,ACh}$ changes during embryonic development. At early stages, $I_{K,ACh}$ is primarily formed by Kir3.1, while in late embryonic and adult cells, Kir3.4 is the predominant subunit. This change in subunit composition results in reduced rectification of $I_{K,ACh}$, allowing for marked K^+ currents over the whole physiological voltage range. As a consequence, $I_{K,ACh}$ is able to generate the membrane hyperpolarization that underlies the strong negative chronotropy occurring in late- but not early-stage atrial cardiomyocytes upon application of muscarinic agonists. Both strong negative chronotropy and membrane hyperpolarization can be induced in early-stage cardiomyocytes by viral overexpression of the mildly rectifying Kir3.4 subunit. Thus, a switch in subunit composition is used to adopt $I_{K,ACh}$ to its functional role in adult cardiomyocytes.

Introduction

Potassium (K^+) channels can be generally classified according to their outward- or inward-rectifying current-voltage (I-V) relation (1). Outward rectification is observed in voltage-gated K^+ (Kv) channels, which are primarily involved in repolarization of the action potential (AP). In contrast, inward-rectifier K^+ (Kir) channels stabilize the membrane potential near the equilibrium potential for K^+ (E_K) in many types of excitable and nonexcitable cells (1). Inward-rectification results from a voltage-dependent block of these channels by the intracellular polyamines spermine and spermidine (2, 3) that occlude the channel pore when K^+ flux is directed outward at potentials positive to E_K. As a consequence, Kir channels display high K^+ conductance around E_K and at a limited voltage range positive to E_K, while at further depolarized potentials channels are blocked, and, therefore, no longer conductive. Accordingly, the voltage range where stabilization of the membrane potential occurs is defined by the strength of the polyamine-block that may be strong or weak and varies among Kir subunits (reviewed in ref. 4).

In cardiac myocytes, several types of Kir channels are expressed, the strong rectifier I_{K1} (5), the ATP-sensitive K^+ channel $I_{K,ATP}$ (6) and the acetylcholine-activated (ACh-activated) K^+ channel ($I_{K,ACh}$) (7). Different from the others, $I_{K,ACh}$ is activated by the Gβγ dimer (8, 9) released from the pertussis toxin–sensitive G protein G_i (10) upon stimulation of the muscarinic type 2 (M2) receptor. $I_{K,ACh}$ is a heterotetramer assembled from Kir3.1 and Kir3.4 subunits (11) and is primarily expressed in sinusoidal and atrial cardiomyocytes. In these cells, release of ACh from parasympathetic nerves leads to negative chronotropy — a phenomenon that results from $I_{K,Ach}$-mediated hyperpolarization of the membrane potential (7, 12). The negative chronotropic effect is further promoted by muscarinic inhibition of L-type calcium channels and hyperpolarization-activated nonselective cation channels (13) that decrease the threshold level and slow diastolic depolarization (14, 15).

In our previous work, the expression, modulation, and functional role of ion channels has been investigated in detail during early stages of development using ES cell–derived cardiomyocytes (reviewed in refs. 16, 17). When we investigated regulation of the spontaneous electrical activity in early-stage cardiomyocytes, we observed that, in contrast to adult cells, the muscarinic agonist carbachol (CCh) had a negative chronotropic effect without prominent hyperpolarization (14). As this result implied lack or low density of $I_{K,ACh}$, we aimed to investigate the functional expression of $I_{K,ACh}$ and its possible involvement in the regulation of chronotropy during early and late embryonic cardiomyogenesis.

Here we provide evidence that $I_{K,ACh}$ is expressed in both early and late stages of embryonic development. The ACh-induced hyperpolarization observed in late-stage and adult cardiomyocytes is shown to be related to the subunit composition of $I_{K,ACh}$.

Results

Muscarinic control of chronotropy changes during embryonic development. APs were recorded from spontaneously beating early-embryonic- (E10.5–E12.5) and late-embryonic-stage (E16.5–E18.5) cardiomyocytes of murine atria. As shown in Figure 1A (upper panel), amplitude and maximal diastolic potential of APs were similar in myocytes of either stage (mean values of 88.6 ± 6.8 mV and –58.2 ± 3.0 mV, n = 10 for early stage; and 86.2 ± 7.2 mV

Nonstandard abbreviations used: ACh, acetylcholine; AP, action potential; CCh, carbachol; EDS, early developmental stage; E_k, equilibrium potential for K^+; $I_{K,ACh}$, Ach-activated K^+ channel(s); I-V, current-voltage; K^+, potassium; Kir, inward-rectifier K^+; Kv, voltage-gated K^+; LDS, late developmental stage; M2, muscarinic type 2.

Conflict of interest: The authors have declared that no conflict of interest exists.

Citation for this article: *J. Clin. Invest.* **114**:994–1001 (2004). doi:10.1172/JCI200415925.

and –56.7 ± 2.3 mV, n = 9 for late stage), while the duration of APs shortened during differentiation.

A striking difference was observed when CCh (1 μM) was applied to the two populations of cardiomyocytes. While a mild negative chronotropy was evoked in early-stage myocytes, decreasing the beating frequency by about 2-fold (n = 8; Figure 1, A–C), a pronounced negative chronotropic effect was observed in all late-stage myocytes, as CCh reduced the beating frequency by more than 10-fold (n = 9; Figure 1, A–C). This chronotropic effect was accompanied by a differential change in membrane potential. Thus, CCh application led to pronounced hyperpolarization in all late-stage myocytes tested (16.2 ± 1.4 mV, n = 9), while only 6 out of 10 early-stage myocytes responded to CCh with hyperpolarization, although with a smaller amplitude (7.9 ± 1.4 mV) (Figure 1, B–D). Similar results for hyperpolarization of membrane potential were obtained with ES cell–derived cardiomyocytes (data not shown). In contrast to atrial myocytes, ventricular cardiomyocytes of either developmental stage did not exhibit membrane hyperpolarization in the presence of CCh (n = 13; Figure 1B).

The correlation between the CCh effect and activation of $I_{K,ACh}$ was further investigated with tertiapin (1 μM), a selective blocker of Kir3 channels (18). As shown in Figure 2A, tertiapin co-applied with CCh effectively reversed both CCh-mediated negative chronotropy (Figure 2B) and membrane hyperpolarization (Figure 2C) in late-stage atrial cardiomyocytes, while only minor effects were observed in early-stage atrial cardiomyocytes (Figure 2C). Sole application of tertiapin only minimally increased basal AP frequency in early- (9.2% ± 5%) and late-stage (12.4% ± 4%, data are mean ± SEM) atrial cells and did not affect at all the membrane potential (n = 5 and n = 3 for early- and late-stage atrial cardiomyocytes, respectively).

$I_{K,ACh}$ is expressed at similar densities at both stages of differentiation. Because of the distinct responses of early- and late-stage atrial cardiomyocytes to CCh, amplitude and activation of $I_{K,ACh}$ at each stage were further investigated. First, maximal $I_{K,ACh}$ elicited by CCh was recorded from early- and late-stage atrial cells at a holding potential of –70 mV in 30 mM external K^+. As shown in Figure 3A, the $I_{K,ACh}$ amplitude was almost identical in either type of cell (current amplitudes of 16.2 ± 1.8 pA/pF, n = 12, and 16.9 ± 3.4 mV, n = 9, for early- and late-stage atrial cardiomyocytes, respectively).

In addition, M2 receptor expression and levels of G_i/G_o proteins were determined in radioligand binding assays and [^{32}P]ADP-ribosylation reactions. While M2 receptor expression differed between early- and late-stage murine-atria (Figure 3B), G_i/G_o proteins linking receptor activity to the downstream signaling cascade were almost identical (Figure 3C). Together, these results suggested that the distinct CCh responses of early- and late-stage atrial cardiomyocytes are not due to different amounts of $I_{K,ACh}$.

Subunit composition of $I_{K,ACh}$ changes during development. We therefore turned to an investigation of the functional properties of $I_{K,ACh}$ activated to steady-state with CCh to exclude any influences of the M2 receptor G protein cascade.

As shown in Figure 4, the time course of $I_{K,Ach}$-mediated currents recorded in response to a voltage step from 0 to –100 mV (see Methods) was distinct in cardiomyocytes of either developmental stage as depicted by representative current traces. Thus, in late-stage atrial myocytes, the onset of current was largely instantaneous, while it was exponential in atrial cardiomyocytes of early stages (Figure 4A, upper panel). Analysis of currents from early-stage myocytes showed that the onset of current was monoexponential, with a time constant (τ_{on}) of 13.9 ± 5.2 ms (mean ± SD of n = 7 cells). In late-stage myocytes, onset of current was either instantaneous (4 out of 8 cells) or exhibited a small exponential component (relative contribution of 0.16 ± 0.06; 4 out of 8 cells) with a τ_{on} of 16.9 ± 4.3 ms (mean ± SD) (Figure 4A, lower panel). The maximal $I_{K,ACh}$ amplitude was almost identical in atria-derived myocytes of both stages (mean ± SEM current density of 39.4 ± 9.4 pA/pF, n = 11 and 47.6 ± 6.3 pA/pF, n = 11, for early and late stages, respectively).

Very similar results were obtained in experiments with ES cell–derived cardiomyocytes (Figure 4B). Early-developmental-

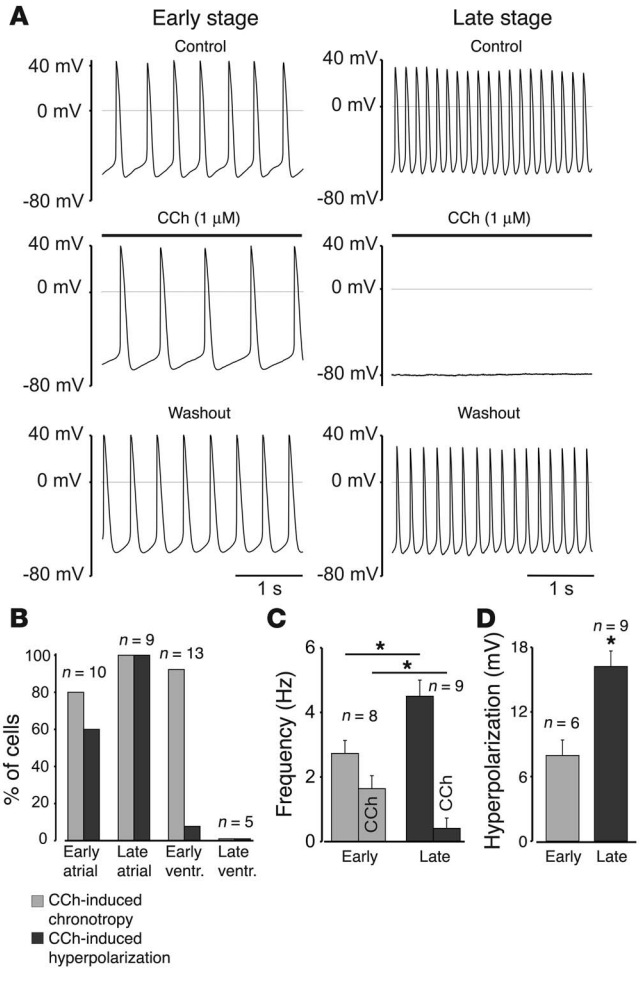

Figure 1
Chronotropy differs between early- and late-stage atrial cardiomyocytes. (**A**) Spontaneous APs are distinctly slowed by CCh (1 μM) in early- (left panel) and late-stage (right panel) cardiomyocytes. APs were recorded under current-clamp conditions; CCh was bath applied. (**B**) Percentage of cells displaying chronotropic effect and membrane hyperpolarization following application of CCh. Note that only 60% of early-stage cells display hyperpolarization upon application of CCh. (**C**) AP frequency of early- and late-stage cardiomyocytes before and after application of CCh; data are mean ± SEM of 8 and 9 experiments (P = 0.016 for control and P = 0.022 for CCh, unpaired Student's t test). (**D**) Hyperpolarization induced by CCh in early and late stage cardiomyocytes; data are mean ± SEM of 6 and 9 experiments, respectively (P = 0.002, unpaired Student's t test). Asterisks denote statistically significant difference.

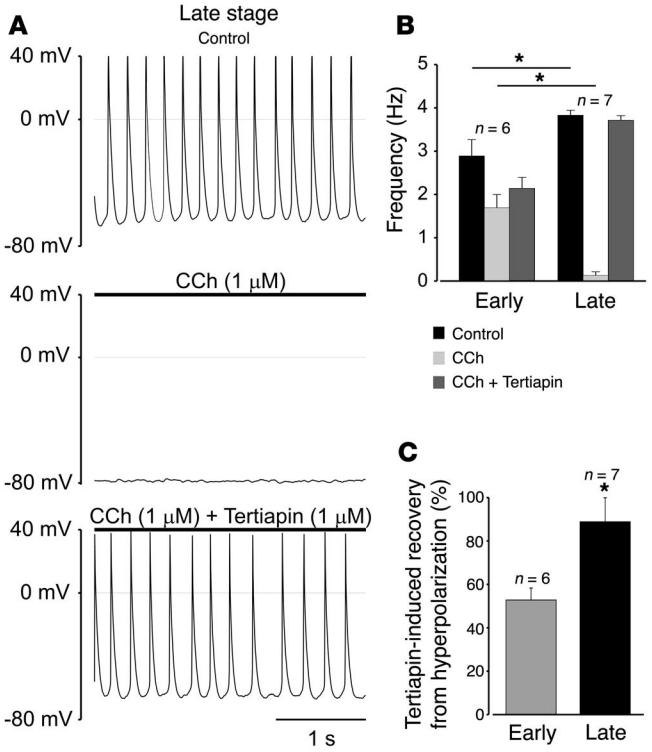

Figure 2
The CCh effect is blocked by the $I_{K,ACh}$ -selective blocker tertiapin. (**A**) Hyperpolarization and negative chronotropy induced by CCh (1 μM) are reversed by tertiapin (1 μM) in a late-stage atrial cardiomyocyte. (**B**) CCh-induced deceleration of spontaneous APs is reversed by tertiapin in late-stage but not in early-stage atrial cardiomyocytes. Data are mean ± SEM of 6 early- and 7 late-stage cells ($P = 0.026$ for control and $P = 0.0003$ for CCh, unpaired Student's t test). (**C**) Tertiapin-induced depolarization of the membrane potential in CCh-treated early- and late-stage atrial cardiomyocytes ($P = 0.0007$, unpaired Student's t test). Recovery was estimated by determining the maximal diastolic potential prior to application of CCh and in presence of CCh and tertiapin. Asterisks denote statistically significant difference.

stage (EDS) cells displayed exponential onset of current (τ_{on} of 15.9 ± 7.3 ms, mean ± SD of $n = 8$ cells), while the majority of late-developmental-stage (LDS) cardiomyocytes (6 out of 9 cells) exhibited instantaneous current onset. Some LDS cells (3 out of 9) displayed intermediate behavior with an I_0/I_{max} ratio of about 0.5 (Figure 4B, lower panel). This was most likely due to the ES cell system, where complete synchronization of differentiation does not occur (16).

Exponential onset of currents mediated by heterologously expressed Kir3.1 and Kir3.4 channels in response to hyperpolarizing voltage steps was shown to reflect unbinding of polyamines from the channel. A negatively charged aspartate residue in the second transmembrane domain of the Kir3.1 subunit was identified as the major structural determinant (19). Neutralization of this residue, as in the Kir3.4 subunit, leads to a largely instantaneous onset of current. We therefore tested whether the distinct character of the onset of $I_{K,ACh}$ observed in early- and in late-stage atria– and ES cell–derived cardiomyocytes may be due to different integration of the Kir3.1 subunit into $I_{K,ACh}$. Various ratios of cRNAs coding for Kir3.1 and Kir3.4 were injected into *Xenopus* oocytes, and the onset of current was measured. As shown in Figure 5A, current onset was largely instantaneous at an excess expression of Kir3.4, while exponential activation became more and more prominent upon increasing the amount of Kir3.1. The relative contribution of the exponential current component decreased from 0.37 ± 0.04 (mean ± SD, $n = 6$) at a Kir3.1/Kir3.4 cRNA ratio of 10:1 to 0.03 ± 0.02 ($n = 4$) at a cRNA ratio of 1:10, respectively (Figure 5, B and C).

These results suggest that the ratio of Kir3.1 and Kir3.4 proteins present in the plasma membrane of atria and ES cell–derived cardiomyocytes may change during embryonic development. This hypothesis was further corroborated by quantitative RT-PCR performed on early- and late-stage atria. As illustrated in Figure 6A for 3 independent experiments, expression of Kir3.4 mRNA is low at early stages and increases markedly during development. In contrast, a marked decrease was observed with Kir3.1 mRNA. Consequently, the Kir3.4/Kir3.1 mRNA ratio increased during cardiac development by more than 600-fold (Figure 6B).

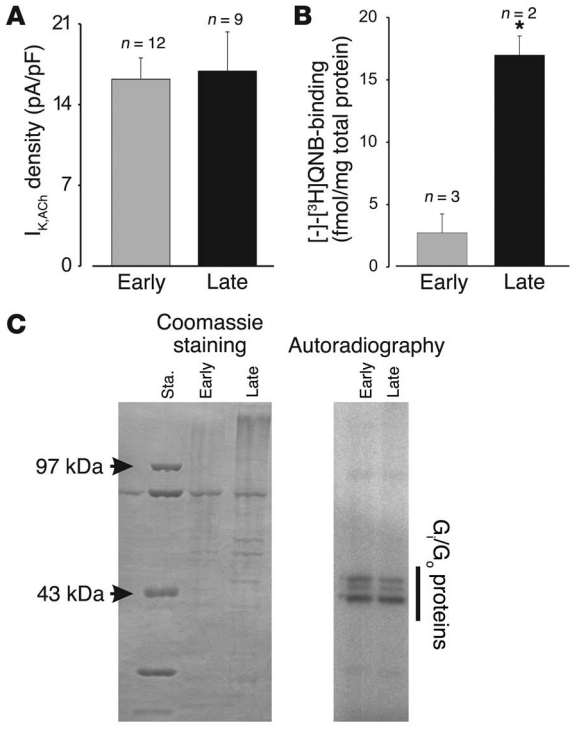

Figure 3
$I_{K,ACh}$ density, M2 receptor expression, and G_i/G_o-protein content in atrial cardiomyocytes during embryonic development. (**A**) Density of $I_{K,ACh}$ determined at a holding potential of –70 mV is identical at the two differentiation stages. Extracellular K^+ was 30 mM, and data are mean ± SEM of 12 early- and 9 late-stage cardiomyocytes ($P = 0.9$, unpaired Student's t test). (**B**) M2 receptor expression in early- and late-stage atria determined from binding experiments with [-]-[^{3}H]QNB. Data are mean ± SD of 3 early- and 2 late-stage cell preparations ($P = 0.002$, unpaired Student's t test). (**C**) G_i/G_o-protein content of atrial membranes determined by [^{32}P]ADP-ribosylation analyzed densitometrically. One of 2 independent experiments with identical results is shown. Comparable protein loading was confirmed with Coomassie staining. Asterisk denotes statistically significant difference. Sta., standard.

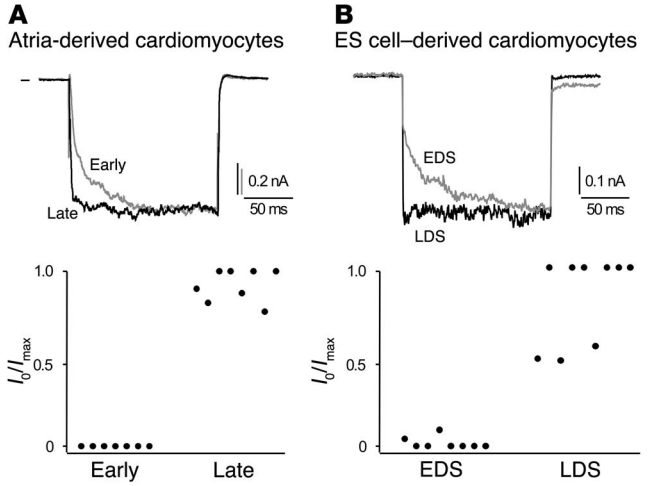

Figure 4
Time course of CCh-induced $I_{K,ACh}$ differs between early- and late-stage cardiomyocytes. (**A** and **B**) Upper panel: $I_{K,ACh}$ recorded in response to a voltage step from 0 to –100 mV under symmetrical K^+ conditions in an early- and late-stage cardiomyocyte derived from atria (**A**) or ES cells (**B**, recorded with perforated patch). Lower panel: relative contribution of the instantaneous component (I_0) to maximal $I_{K,ACh}$ amplitude (I_{max}) as measured in individual early- and late-stage cardiomyocytes derived from atria (**A**) or ES cells (**B**).

Rectification of $I_{K,ACh}$ is altered by the change in subunit composition during development. Next, we investigated the rectification properties of $I_{K,ACh}$ in early- and late-stage atrial cardiomyocytes as well as of Kir channels formed in oocytes upon injection of Kir3.1 and Kir3.4 cRNAs at ratios of 1:10 and 10:1.

As shown in the steady-state I-V relations, rectification is strong in early-stage myocytes, with complete block of outward currents at potentials greater than or equal to 25 mV (Figure 7, A and B) positive to E_K (0 mV at symmetrical K^+ conditions). In contrast, late-stage cardiomyocytes exhibited less pronounced rectification, allowing for significant outward currents over the whole potential range positive to E_K (Figure 7, A and B). These outward currents were K^+ currents through $I_{K,ACh}$ rather than leakage, as inwardly directed currents at potentials negative to E_K were completely blocked by external Cs^+ in a voltage-dependent manner, a feature characteristic of Kir channels (20) (Figure 7D). Similarly, distinct rectification was obtained with early- and late-stage atrial cardiomyocytes when $I_{K,ACh}$ was activated with GTP-γ-S (0.3 mM, added to the patch pipette) instead of CCh that bypassed the M2 receptor cascade (n = 4 and 3 cells, respectively).

Distinct rectification properties were also observed with heterologously expressed $I_{K,ACh}$. Kir channels resulting from a Kir3.1/Kir3.4 cRNA ratio of 10:1 showed strong rectification with blocking of outward currents for potentials positive to E_K, while channels forming upon excess injection of Kir3.4 cRNA (Kir3.1/Kir3.4 ratio of 1:10) conducted K^+ currents over the whole voltage range tested (Figure 7C).

These results strongly suggest that the differences in rectification observed with $I_{K,ACh}$ in early- and late-stage cardiomyocytes are due to changes in its subunit composition.

Overexpression of Kir3.4 in early-stage cardiomyocytes restores biophysical and functional features of late-stage cells. Kir3.4 and Kir3.1 subunits were overexpressed in early- and late-stage atrial cardiomyocytes in order to further explore whether the difference in rectification resulting from a developmental change in subunit composition of $I_{K,ACh}$ is related to the distinct CCh-induced negative chronotropy and membrane hyperpolarization. As shown in Figure 8A, early-stage cells overexpressing Kir3.4 exhibited $I_{K,ACh}$ with largely instantaneous onset and weak rectification (n = 8) similar to that observed in nontransfected late-stage atrial cardiomyocytes. In contrast, when Kir3.1 was overexpressed in late-stage atrial cardiomyocytes, $I_{K,ACh}$ displayed an exponential onset of current together with strong inward rectification (n = 5; Figure 8B).

Moreover, when CCh (1 μM) was applied to Kir3.4-transfected early-stage atrial cardiomyocytes, a prominent negative chronotropic effect was observed in all cells tested, accompanied by a hyperpolarization of the membrane potential (13.3 ± 1.4 mV; mean ± SEM, n = 9; Figure 8, C and D). Both hyperpolarization and negative chronotropy were reversed by tertiapin (n = 9; Figure 8, C and D), as seen before in late-stage cells (Figure 2, B and C). Interestingly, Kir3.4 overexpressing early-stage cells displayed significantly augmented beating frequencies (4.4 ± 0.3 Hz, n = 9; Figure 8D) compared with the untransfected controls (Figure 1C, P = 0.004; Figure 2B, P = 0.006, unpaired Student's t test). Together, these results indicate that Kir3.4-dominant $I_{K,ACh}$ is both necessary and sufficient for reconstituting a late-stage phenotype in early-stage atrial cardiomyocytes with respect to membrane hyperpolarization and negative chronotropy induced by muscarinic receptor stimulation.

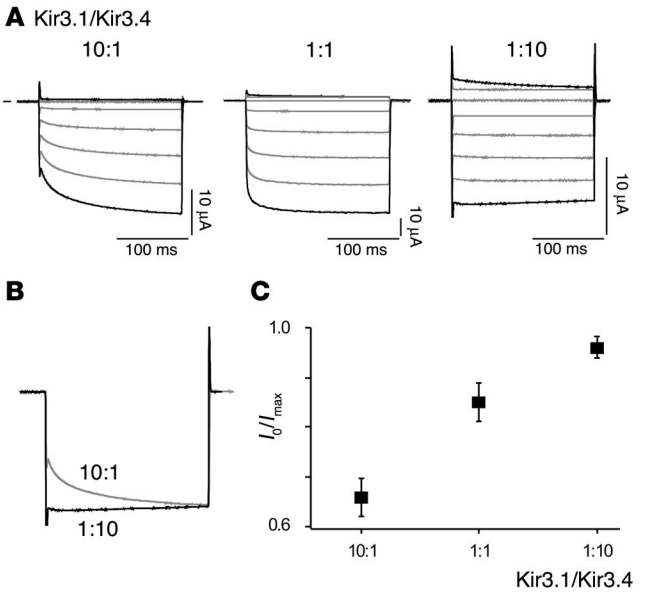

Figure 5
Onset of current through recombinant $I_{K,ACh}$ changes with the Kir3.1/Kir3.4 cRNA ratio. (**A**) Currents recorded from whole oocytes injected with the cRNAs indicated in response to voltage steps from 0 mV to potentials between –100 mV and 40 mV (increments of 20 mV); current and time scaling is 10 μA and 100 ms throughout. (**B**) Overlay of current responses obtained at –100 mV from oocytes injected with Kir3.1/Kir3.4 cRNA at a ratio of 10:1 (gray trace) or 1:10 (black trace). Note the difference in time course (τ_{on} of 16.6 ± 1.6 ms, n = 5; and 17.5 ± 3.9 ms, n = 4 for the 1:10 and 10:1 ratios, respectively). (**C**) I_0/I_{max} ratio as in Figure 4 measured in oocytes injected with Kir3.1 and Kir3.4 cRNA at the ratios indicated. Data are mean ± SD of 4–6 oocytes.

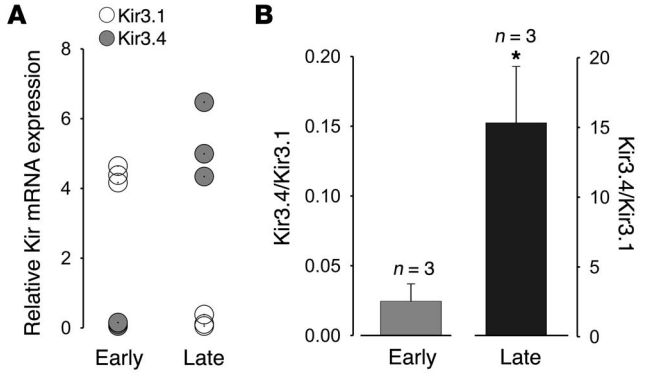

Figure 6
Amount of Kir3.1 and Kir3.4 mRNA changes during embryonic development in atria. (**A**) Quantitative RT-PCR (Taqman) performed on early- (E11.5) and late-stage (E18.5) embryonic atria. mRNA levels in the different samples were normalized to 18S rRNA. Data are obtained from 3 independent RNA preparations. (**B**) Ratio of Kir3.4/Kir3.1 mRNA in early- and late-stage atria as determined from the data in **A**. Data are mean ± SD ($P = 0.003$, unpaired Student's t test). Asterisk denotes statistically significant difference.

Discussion

The results presented show that the G protein–activated K^+ channel $I_{K,ACh}$ changes its molecular composition in cardiomyocytes during embryonic development: while the strongly rectifying Kir3.1 dominates at early stages, late-stage and adult $I_{K,ACh}$ is made up mainly of the mildly rectifying Kir3.4 subunit. As a consequence, rectification of $I_{K,ACh}$ is reduced at late stages of embryonic development, which allows for a marked K^+ conductance over the whole voltage range positive to E_K. Accordingly, $I_{K,ACh}$ activated by Ach released from the vagal nerve leads to hyperpolarization of the membrane potential, which in turn shunts excitation and largely reduces electrical activity (AP frequency) (Figure 1). This negative chronotropic effect does not occur in early-stage myocytes, since Kir3.1-dominated $I_{K,ACh}$ is blocked by polyamines at the maximal diastolic potential and, therefore, is unable to provide additional K^+ conductance upon vagal stimulation.

The correlation between the distinct rectification properties of the two Kir subunits and the distinct reaction of early- and late-stage atrial cells on muscarinic agonists was most obvious in viral transfection experiments. Thus, exogenous expression of Kir3.4 restored the negative chronotropic effect in early-stage cardiomyocytes (Figure 8). The latter result further implied that early-stage cardiomyocytes dispose of all the signaling elements required for M2-induced activation of $I_{K,ACh}$.

As structural correlates for the distinct rectification properties observed among the various Kir channels, a number of sites have been identified that govern the interaction between the Kir channel pores and polyamines (4, 21). Among these, a residue in the second transmembrane helix was found to be particularly effective and to discriminate between strong and weak rectifiers. Strong rectifiers bear a negatively charged residue, while weak rectifiers present with a neutral amino acid at this position (22–24). Kir3.1 exhibits an aspartate residue at this site (D173), while an asparagine residue is found in Kir3.4 (N179). Accordingly, the more Kir3.1 subunits are integrated into an $I_{K,ACh}$ channel, the more prominent its rectification should be (25–27). This was indeed observed in heterologous expression experiments in which the ratios of Kir3.1 and Kir3.4 cRNA were varied between 10:1 and 1:10 (see Figures 4 and 7). The close agreement between the properties of $I_{K,ACh}$ and heterologously expressed Kir3.1 and Kir3.4 channels strongly suggested that the ratio of Kir3.1/Kir3.4 subunits changes during embryonic development. This conclusion is further supported by quantitative PCR reported in Figure 6 as well as a report by Corey and Clapham (28) demonstrating that Kir3.4 is the predominant $I_{K,ACh}$ subunit in adult atria. Whether this reported change in composition of $I_{K,ACh}$ is due to an altered subunit stoichiometry of Kir3.1/Kir3.4 heteromultimers or due to an increase of Kir3.4 homomeric channels (28) presently remains unclear.

So far, a change in subunit composition during development has been reported only for the nicotinic ACh receptor. However, in contrast to our findings on $I_{K,ACh}$, nicotinic ACh receptors exchange their embryonic γ subunit for the adult ε subunit (29–31). This subunit exchange has been found to be accompanied by biophysical modifications, in particular an increase in the mean open time and prolongation of burst lengths (32).

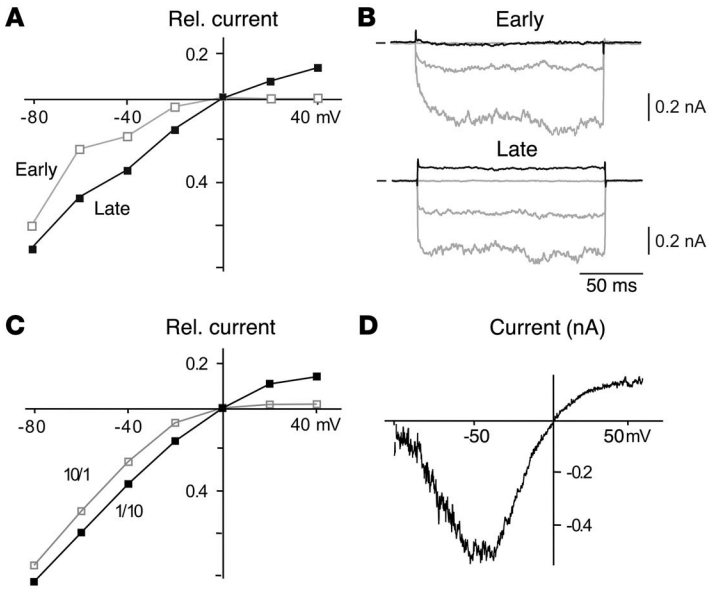

Figure 7
Rectification of $I_{K,ACh}$ decreases during cardiac development. (**A**) Steady-state I-V relation of $I_{K,ACh}$ (voltage steps from –80 mV to 40 mV in 20-mV steps) determined in early- (open squares) and late-stage (filled squares) atria-derived cardiomyocytes. Rel. current, relative current. (**B**) Original $I_{K,Ach}$-mediated currents induced by CCh and recorded at potentials of –80, –40, 0 mV (gray traces) and 40 mV (black trace) in early- and late-stage atria-derived cardiomyocytes; short lines indicate zero current. Note the difference in outward current amplitude. (**C**) Steady-state I-V relation determined in oocytes injected with Kir3.1 and Kir3.4 cRNA at the ratios indicated. (**D**) $I_{K,Ach}$-mediated current recorded in a late-stage ES cell–derived cardiomyocyte (recorded with perforated patch) in response to a 500 ms voltage ramp from –100 to 60 mV under symmetrical K^+ conditions with 100 μM Cs^+ present in the bath medium. Note complete block of channels by Cs^+ at –100 mV.

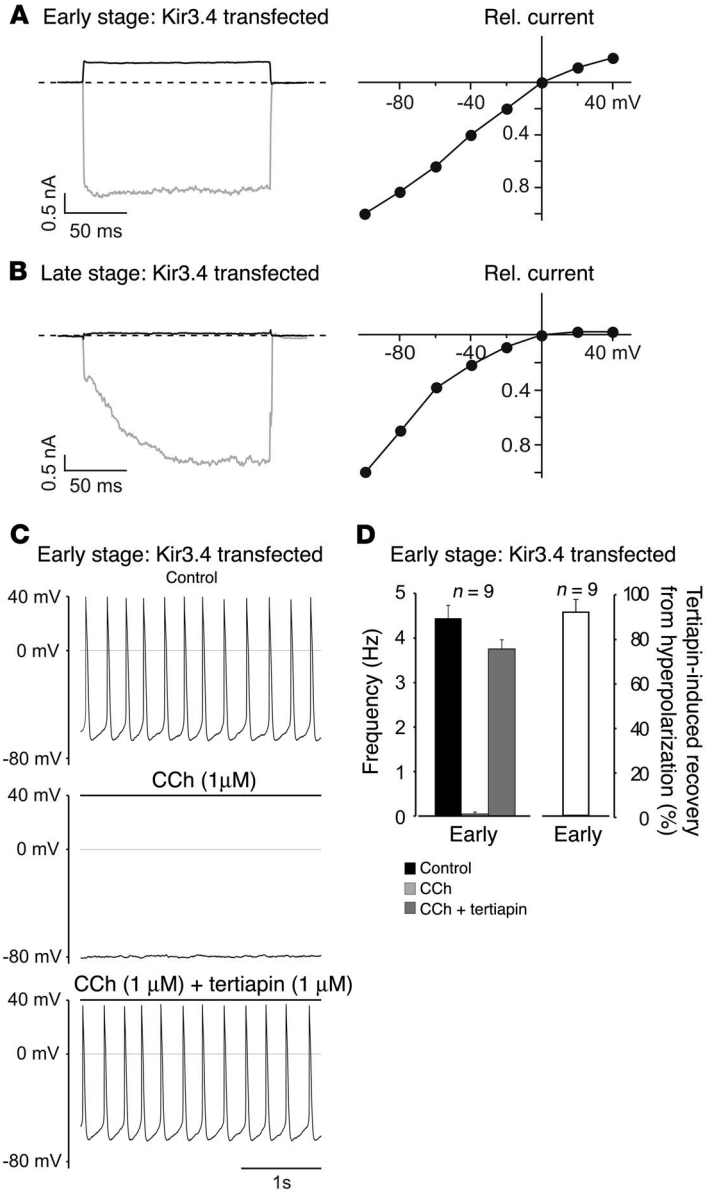

Figure 8
Overexpression of Kir3.4 in early-stage atrial cardiomyocytes reconstitutes the late-stage phenotype. (**A**) Left panel: $I_{K,ACh}$-mediated currents induced by CCh and recorded at potentials of –100 mV (gray trace) and 40 mV (black trace) in an early-stage cell overexpressing Kir3.4. Right panel: Steady-state I-V relation of the experiment in **A** (voltage steps from –100 mV to 40 mV in 20-mV steps). (**B**) Current traces and steady-state I-V relation as in **A**, but recorded from a late-stage cardiomyocyte overexpressing Kir3.1. (**C**) Hyperpolarization and negative chronotropy induced by CCh and reversed by tertiapin in an early-stage Kir3.4–overexpressing cardiomyocyte. (**D**) CCh-induced deceleration of spontaneous APs (left axis) and reversal by tertiapin (right axis) in early-stage cardiomyocytes overexpressing Kir3.4. Data are mean ± SEM of 9 cells.

It is tempting to speculate that changes occurring in subunit composition of ion channels resulting in altered function may represent a more general motif of adaptation during development. Moreover, since pathologically altered cells can recapitulate their embryonic phenotype, similar changes may also occur in diseased cells.

Methods

Harvest and isolation of embryonic cardiomyocytes. For harvesting embryonic cardiomyocytes from murine atria, mice of the strain HIM:OF1 were bred using superovulation for precise staging (33). For isolation of early- and late-stage cardiomyocytes, E10.5–E12.5 and E16.5–E18.5 embryos were used, respectively. After embryos were harvested, hearts were dissected and atria separated from ventricles. For experiments with ES cells, the cell line D3 was used. ES cells were differentiated into cardiomyocytes, as described previously (34). EDS and LDS cells were obtained from embryoid bodies plated for 3–4 days and 9–12 days, respectively. Single cardiomyocytes were isolated from murine embryonic atria as well as from clusters of spontaneously beating areas of embryoid bodies using enzymatic dissociation procedures as described previously (14). The isolated cells were plated on sterile, gelatin-coated glass coverslips and kept in the incubator for 24–48 hours. Spontaneously contracting cardiomyocytes could be observed within 12 hours after cell preparation. The experiments using mouse tissue were approved by the local ethical committee (University of Cologne).

Electrophysiology on cardiomyocytes. Isolated, spontaneously beating atrial or ES cell–derived cardiomyocytes were investigated with the whole-cell patch clamp technique in conventional (atria-derived murine cells) or perforated configuration (ES cell–derived cardiomyocytes; for details, see ref. 35). For recordings, an Axopatch 200 A (Axon Instruments) or an EPC 9 amplifier (HEKA) were used. Data were digitized at 10 kHz, filtered at 1 kHz, and stored on hard drive. Steady-state $I_{K,ACh}$ was recorded at a holding potential of –70 mV. I-V relations were determined by subtracting currents recorded in the presence and absence of CCh either in response to voltage steps (from –100 mV to 40 mV with 20-mV increments, 150 ms, holding potential 0 mV) or voltage-ramps (–100 mV to 80 mV in 150 ms or –100 mV to 60 mV in 500 ms). Data are given as mean ± SD or SEM, as indicated. For quantification of activation kinetics, currents recorded in response to voltage steps were fitted with monoexponentials. The respective time constant is given as τ_{act}; the value for I_0 was determined by subtracting the exponential current component (extrapolation of the fitted exponential to time point $t = 0$) from I_{max} obtained as asymptotic of the exponential fit. Statistical analysis was performed using unpaired Student's t test.

All experiments were performed at 37°C. Solutions for current-clamp recordings had the following composition: 50 mM KCl, 80 mM Kaspartate, 1 mM $MgCl_2$, 3 mM MgATP, 10 mM EGTA, 10 mM HEPES, pH 7.4 (internal solution; pH adjusted with KOH); 140 mM NaCl, 5.4 mM KCl, 3.6 mM $CaCl_2$, 1 mM $MgCl_2$, 10 mM HEPES, 10 mM glucose, pH 7.4 (external solution; pH adjusted with NaOH). For voltage clamp experiments, solutions were: 40 mM KCl, 100 mM Kaspartate, 5 mM MgATP, 2 mM EGTA, 0.01 mM GTP, 10 mM HEPES, pH 7.4 (internal solution; pH adjusted with KOH); 140 mM KCl, 2 mM $MgCl_2$, 5 mM NaCl, 1.8 mM $CaCl_2$, 5 mM glucose, 5 mM HEPES, pH 7.4 (external solution; pH adjusted with KOH). Steady-state recordings were performed in 30 mM extracellular K^+. For perforated patch-clamp experiments in ES cell–derived cardiomyocytes the internal solution was: 55 mM KCl, 7 mM $MgCl_2$, 70 mM K_2SO_4,10 mM HEPES, pH 7.4 (adjusted with KOH); the final concentration of amphotericin was 450 μg/ml. The external solution was: 140 mM KCl, 5 mM NaCl, 2 mM $MgCl_2$, 1.8 mM $CaCl_2$, 5 mM glucose, 5 mM HEPES, pH 7.4 (adjusted with KOH). Most of the voltage clamp recordings of

$I_{K,ACh}$ were performed in equimolar K^+ to increase current amplitude. All test substances were purchased from Sigma-Aldrich and were dissolved in extracellular or pipette (GTP-γ-S) solution prior to use.

RNA extraction and cDNA synthesis. Total RNA was isolated from embryonic heart at different stages (E11.5, E18.5) using the RNA isolation kit from Qiagen. The extracted RNA was quantified with a spectrophotometer. One microgram of RNA was used for reverse transcription into cDNA using random hexamers (Roche Diagnostics) as primers and SuperscriptII Reverse Transcriptase (Invitrogen) following the manufacturer's instructions. cDNA samples were stored at –20°C.

Quantitative real-time PCR. The mRNA levels of Kir3.1 and Kir3.4 as well as of 18S rRNA (as an endogenous control) were quantified by real-time PCR analysis (TaqMan chemistry; Applied Biosystems) on an ABI Prism 7700 sequence detection system (Applied Biosystems). All primers (see below) were designed with Primer Expresss 1.5 software (Applied Biosystems). Quantitative real-time PCR was performed in a total reaction volume of 25 μl containing 12.5 μl Taqman Universal Master Mix at a concentration of ×2, 2.25 pM of each forward and reverse primer, and 0.75 pM dual-labeled fluorogenic internal probe in MicroAmp optical 96-well plates covered with MicroAmp optical caps (Applied Biosystems). 0.5 μl cDNA template was added to the mixture for amplification of Kir3.1 and Kir3.4, while 2 nl cDNA was used for 18S rRNA quantification. The PCR was carried out using the following cycling parameters: 50°C for 2 minutes and then 95°C for 10 minutes, followed by 40 cycles of 95°C for 15 seconds and 60°C for 1 minute.

For quantification of Kir3.1 and Kir3.4 expression relative to that of 18S rRNA, the input cDNA levels were calculated from cycle number values (×10 the standard deviation of base-line emissions measured from cycles 3 to 15) provided by standard curves (linear plots of fluorescence versus cycle number) that were prepared from serial dilutions of early- (Kir3.1) and late-stage (Kir3.4) samples according to standard procedures (36).

Sequences of the primers or probes were the following: Kir3.1 forward primer (5′-CTGCGCAACAGCCACATG-3′); Kir3.1 reverse primer (5′-CCTCAGGTGTCTGCCGAGAT-3′); Kir3.1 probe (FAM-5′-CCGCGCAGATCCGCTGCA-3′-TAMRA); Kir3.4 forward primer (5′-TCTGAAACAGCACTTCTTGCTTAAG-3′); Kir3.4 reverse primer (5′-CCATGTCTTGATTCATAGCATTCC-3′); Kir3.4 probe (5′-CCATCTAGCAAGCAGATGGCCGGT-3′). The Kir3.4 probe used in the TaqMan reactions was designed to have nonfluorescent quenchers and minor groove-binding modifications.

Electrophysiology on recombinant $I_{K,ACh}$. Oocyte handling and injection of cRNA specific for Kir3.1 and Kir3.4 was done as described previously (3). Electrophysiological recordings were performed 3–7 days after injection using a 2-microelectrode voltage clamp. For 2-microelectrode recordings, current and voltage electrodes were pulled from thick-walled borosilicate glass and had resistances between 0.1 and 0.5 MΩ when filled with 3 M KCl. Currents were recorded with a TurboTec 01C amplifier (npi electronic GmbH), digitized at 10 kHz (ITC-16, HEKA) and stored on hard drive. The bath solution was composed as follows: 117.5 mM KCl, 1.8 mM $CaCl_2$, 10 mM HEPES (pH adjusted to 7.2 with KOH). All experiments were performed at room temperature (approximately 23°C). I-V relations (Figure 5A) were obtained by plotting the steady-state current measured at voltages between –100 and 60 mV (increments of 20 mV) versus the command voltage; τ_{act} and I_0 were determined as described above. Computational work was done on a Macintosh PowerPC using commercial software (IGOR; WaveMetrics) for fitting.

Membrane preparation and radioligand binding assay. Binding assays were carried out with membrane homogenates prepared from atrial tissue essentially as described previously (37). Membrane homogenates were incubated for 3 hours at 22°C in 25 mM sodium phosphate (pH 7.4) containing 5 mM $MgCl_2$. Saturation binding experiments were carried out with (-)-[^{3}H]*N*-quinuclidinyl benzilate ([-]-[^{3}H]QNB; 42.0 Ci/mmol; NEN Life Science Products). Binding was performed with saturating concentrations of the radioligand (2 nM), and nonspecific binding was defined as binding in the presence of 2.5 μM atropine. Protein concentrations were determined by the Bradford method.

[^{32}P]ADP-ribosylation reactions. Membranes in 10 μl were [^{32}P]ADP-ribosylated for 30 minutes at 32°C with preactivated pertussis toxin at 10 μg/ml and 1 μM [^{32}P]$NADP^+$ (2–4 × $10P^{6P}$ cpm) in a final volume of 30 μl as described (38). The reactions were stopped by the addition of 2× Laemmli's sample buffer containing 10 mM $NADP^+$. Aliquots of these mixtures were placed directly into the sample wells of polyacrylamide gels and subjected to 4–8 M urea gradient/9% polyacrylamide gel electrophoresis as described previously (39). After electrophoresis, the slabs were stained with Coomassie blue, destained, dried, and autoradiographed with a Phosphor-Imager (Fuji).

Transfection of embryonic cardiomyocytes. For transfection of atria-derived early- and late-stage cardiomyocytes with rat Kir3.4 or mouse Kir3.1 cDNA (kindly provided by Y. Kurachi, Osaka University, Osaka, Japan) the p-Ad-Track-CMV vector containing the enhanced green fluorescent protein as reporter was used (kindly provided by B. Vogelstein, Johns Hopkins University, Baltimore, Maryland, USA). For transfection, cells were plated on gelatin-coated coverslips and transfected with rat Kir3.4 or mouse Kir3.1 (for details, see also ref. 40) using the Effectene Transfection kit (Qiagen) according to the manufacturer's instructions. Enhanced green fluorescent protein–positive cells were detected about 36 hours after transfection and used for electrophysiological experiments 48 hours after transfection.

Acknowledgments

The authors thank M. Faulhaber, B. Hops, and C. Böttinger for help in cell culture work. We are also grateful to K. Spicher for helping with the ADP-ribosylation experiments and R. Küppers for advice with quantitative PCR. This work was supported by grants from the Deutsche Forschungsgemeinschaft (2089/3-1 to J. Hescheler and 273/3-1 to B.K. Fleischmann).

Received for publication May 14, 2002, and accepted in revised form August 10, 2004.

Address correspondence to: Bernd K. Fleischmann, Institute of Physiology I, University of Bonn, D-53115 Bonn, Germany. Phone: 49-228-73-2403; Fax: 49-228-73-2408; E-mail: bernd.fleischmann@uni-bonn.de.

Nibedita Lenka's present address is: National Centre for Cell Science, Pune University Campus, Pune, Maharashtra, India.

Serge Viatchenko-Karpinski's present address is: Department of Physiology, Texas Tech University Health Sciences Center, Lubbock, Texas, USA.

Bernd K. Fleischmann and Yaqi Duan contributed equally to this work.

1. Hille, B. 2001. *Ion channels of excitable membranes*. Sinauer Associates, Inc. Sunderland, Massachusetts, USA. 814 pp.
2. Lopatin, A.N., Makhina, E.N., and Nichols, C.G. 1994. Potassium channel block by cytoplasmic polyamines as the mechanism of intrinsic rectification. *Nature*. **372**:366–369.
3. Fakler, B., et al. 1995. Strong voltage-dependent inward rectification of inward rectifier K+ channels is caused by intracellular spermine. *Cell*. **80**:149–154.
4. Nichols, C.G., and Lopatin, A.N. 1997. Inward rectifier potassium channels. *Annu. Rev. Physiol.* **59**:171–191.
5. Sakmann, B. and Trube, G. 1984. Conductance properties of single inwardly rectifying potassium

channels in ventricular cells from guinea-pig heart. *J. Physiol.* **347**:641–657.
6. Noma, A. 1983. ATP-regulated K+ channels in cardiac muscle. *Nature.* **305**:147–148.
7. Sakmann, B., Noma, A., and Trautwein, W. 1983. Acetylcholine activation of single muscarinic K+ channels in isolated pacemaker cells of the mammalian heart. *Nature.* **303**:250–253.
8. Wickman, K.D., et al. 1994. Recombinant G-protein beta gamma-subunits activate the muscarinic-gated atrial potassium channel. *Nature.* **368**:255–257.
9. Krapivinsky, G., Krapivinsky, L., Wickman, K., and Clapham, D.E. 1995. G beta gamma binds directly to the G protein-gated K+ channel, IKACh. *J. Biol. Chem.* **270**:29059–29062.
10. Sowell, M.O., et al. 1997. Targeted inactivation of alphai2 or alphai3 disrupts activation of the cardiac muscarinic K+ channel, IKACh, in intact cells. *Proc. Natl. Acad. Sci. U. S. A.* **94**:7921–7926.
11. Krapivinsky, G., et al. 1995. The G-protein-gated atrial K+ channel IKACh is a heteromultimer of two inwardly rectifying K+-channel proteins. *Nature.* **374**:135–141.
12. Taniguchi, J., Noma, A., and Irisawa, H. 1983. Modification of the cardiac action potential by intracellular injection of adenosine triphosphate and related substances in guinea pig single ventricular cells. *Circ. Res.* **53**:131–139.
13. DiFrancesco, D. 1993. Pacemaker mechanisms in cardiac tissue. *Annu. Rev. Physiol.* **55**:455–472.
14. Ji, G.J., et al. 1999. Regulation of the L-type Ca2+ channel during cardiomyogenesis: switch from NO to adenylyl cyclase-mediated inhibition. *FASEB J.* **13**:313–324.
15. Abi-Gerges, N., et al. 2000. Functional expression and regulation of the hyperpolarization activated non selective cation current in embryonic stem cell-derived cardiomyocytes. *J. Physiol.* **523**:377–389.
16. Hescheler, J., et al. 1997. Embryonic stem cells: a model to study structural and functional properties in cardiomyogenesis. *Cardiovasc. Res.* **36**:149–162.
17. Hescheler, J., et al. 1999. Establishment of ionic channels and signalling cascades in the embryonic stem cell-derived primitive endoderm and cardiovascular system. *Cells Tissues Organs.* **165**:153–164.
18. Jin, W., and Lu, Z. 1998. A novel high-affinity inhibitor for inward-rectifier K+ channels. *Biochemistry.* **37**:13291–13299.
19. Lancaster, M.B., et al. 2000. Residues and mechanisms for slow activation and Ba+ block of the cardiac muscarinic K+ channel, Kir3.1/Kir3.4. *J. Biol. Chem.* **275**:35831–35839.
20. Kubo, Y., Reuveny, E., Slesinger, P.A., Jan, Y.N., and Jan, L.Y. 1993. Primary structure and functional expression of a rat G-protein-coupled muscarinic potassium channel. *Nature.* **364**:802–806.
21. Oliver, D., Baukrowitz, T., and Fakler, B. 2000. Polyamines as gating molecules of inward-rectifier K+ channels. *Eur. J. Biochem.* **267**:5824–5829.
22. Fakler, B., et al. 1994. A structural determinant of differential sensitivity of cloned inward rectifier K+ channels to intracellular spermine. *FEBS Lett.* **356**:199–203.
23. Stanfield, P.R., et al. 2001. A single aspartate residue is involved in both intrinsic gating and blockage by Mg2+ of the inward rectifier, IRK1. *J. Physiol.* **478**:1–6.
24. Lu, Z., and MacKinnon, R. 1994. Electrostatic tuning of Mg2+ affinity in an inward-rectifier K+ channel. *Nature.* **371**:243–246.
25. Glowatzki, E., et al. 1995. Subunit-dependent assembly of inward-rectifier K+ channels. *Proc. R. Soc. Lond. B Biol. Sci.* **261**:251–261.
26. Shyng, S., and Nichols, C.G. 1997. Octameric stoichiometry of the KATP channel complex. *J. Gen. Physiol.* **110**:655–664.
27. Yang, J., Jan, Y.N., and Jan, L.Y. 1995. Determination of the subunit stoichiometry of an inwardly rectifying potassium channel. *Neuron.* **15**:1441–1447.
28. Corey, S., and Clapham, D.E. 1998. Identification of native atrial G-protein-regulated inwardly rectifying K+ (GIRK4) channel homomultimers. *J. Biol. Chem.* **273**:27499–27504.
29. Witzemann, V., Barg, B., Nishikawa, Y., Sakmann, B., and Numa, S. 1987. Differential regulation of muscle acetylcholine receptor gamma- and epsilon-subunit mRNAs. *FEBS Lett.* **223**:104–112.
30. Witzemann, V., Barg, B., Criado, M., Stein, E., and Sakmann, B. 1989. Developmental regulation of five subunit specific mRNAs encoding acetylcholine receptor subtypes in rat muscle. *FEBS Lett.* **242**:419–424.
31. Kues, W.A., Sakmann, B., and Witzemann, V. 1995. Differential expression patterns of five acetylcholine receptor subunit genes in rat muscle during development. *Eur. J. Neurosci.* **7**:1376–1385.
32. Franke, C., Koltgen, D., Hatt, H., and Dudel, J. 1992. Activation and desensitization of embryonic-like receptor channels in mouse muscle by acetylcholine concentration steps. *J. Physiol.* **451**:145–158.
33. Fleischmann, M., et al. 1998. Cardiac specific expression of the green fluorescent protein during early murine embryonic development. *FEBS Lett.* **440**:370–376.
34. Maltsev, V.A., Wobus, A.M., Rohwedel, J., Bader, M., and Hescheler, J. 1994. Cardiomyocytes differentiated in vitro from embryonic stem cells developmentally express cardiac-specific genes and ionic currents. *Circ. Res.* **75**:233–244.
35. Viatchenko-Karpinski, S., et al. 1999. Intracellular Ca^{2+} oscillations drive spontaneous contractions in cardiomyocytes during early development. *Proc. Natl. Acad. Sci. U. S. A.* **96**:8259–8264.
36. Liss, B., et al. 2001. Tuning pacemaker frequency of individual dopaminergic neurons by Kv4.3L and KChip3.1 transcription. *EMBO J.* **20**:5715–5724.
37. Dorje, F., et al. 1991. Antagonist binding profiles of five cloned human muscarinic receptor subtypes. *J. Pharmacol. Exp. Ther.* **256**:727–733.
38. Hsu, W.H., et al. 1990. Molecular cloning of a novel splice variant of the alpha subunit of the mammalian Go protein. *J. Biol. Chem.* **265**:11220–11226.
39. Codina, J., Grenet, D., Chang, K.J., and Birnbaumer, L. 1991. Urea gradient/SDS-PAGE; a useful tool in the investigation of signal transducing G proteins. *J. Recept. Res.* **11**:587–601.
40. Bender, K., et al. 2001. Overexpression of monomeric and multimeric GIRK4 subunits in rat atrial myocytes removes fast desensitization and reduces inward rectification of muscarinic K^+ current $I_{K(ACh)}$. Evidence for functional homomeric GIRK4 channels. *J. Biol. Chem.* **276**:28873–28880.